SUPPLEMENTAL INFORMATION - Methods

Anti-influenza H7 human monoclonal antibody H7-200 targets a novel antigenic site in the hemagglutinin head domain interface

Jinhui Dong[1,*], Iuliia Gilchuk[1,*], Sheng Li[2], Ryan Irving[1], Matthew T. Goff[1], Hannah L. Turner[3], Andrew B. Ward[3], Robert H. Carnahan[1,4], James E. Crowe, Jr.[1,4,5]

Methods

Research subject. A blood sample from a survivor of natural H7N9 infection, in a case that was described previously (1) was collected after written informed consent approximately 11 months after recovery from infection. The study was approved by the Institutional Review Board of Vanderbilt University Medical Center.

Cell lines and viruses. The reverse-genetics-derived virus with the H7N9 HA and NA genes on a PR8 backbone, designated A/Shanghai/2/2013 (H7N9)-PR8-IDCDC-RG32A (Influenza Reagent Resource**,** FR-1389), was propagated in embryonated chicken eggs and manipulated under BSL-2 conditions with BSL-3 practices. Virus titration and neutralization assays were performed on MDCK (ATCC, CCL-34) epithelial cells. Cells were determined to be mycoplasma-free at laboratory passage 2, and monthly when in use.

Recombinant protein expression and purification. A cDNA encoding H7N9 (Shanghai/2013) hemagglutinin HA1 (residue 1 – 320, cognate signal peptide included) and a 6-his tag was synthesized (Genscript) and cloned into pcDNA3.1 $^{(+)}$ (ThermoFisher; catalog number: V79020). For the expression of recombinant H7-200 Fab, nucleotide sequences of antibody heavy- and light-chain antibody variable genes were codon-optimized for mammalian expression and synthesized at Twist Biosciences. Resulting gene fragments were directly cloned at Twist Biosciences into the pTwist CMV BetaGlobin WPRE NEO mammalian expression vector (Twist Biosciences) The H7N9 HA1 construct and H7-200 heavy/light chain constructs were used to transfect Expi293F (ThermoFisher Scientific, A14528) cells transiently, and supernatants were harvested after culturing for 6 to 7 days. H7N9 HA1 protein was purified from the supernatants by nickel affinity chromatography with HisTrap Excel columns (GE Healthcare Life Sciences). Recombinant Fab H7-200 was purified with Anti-CH1 CaptureSelect column (GE Healthcare Life Sciences). H7-200 IgG produced by correspondent hybridoma cell line to serum-free medium (GIBCO Hybridoma-SFM, Thermo Fisher Scientific) was purified by affinity chromatography using HiTrap MabSelectSure column (GE Healthcare Life Sciences).

H7-200 antibody isolation. A human hybridoma cell line secreting mAb H7-200 was generated using methods as described previously (2). Briefly, human B cells in the peripheral blood mononuclear cell suspension were immortalized by transformation with Epstein Barr virus in the presence of CpG10103, cyclosporin A and a Chk2 inhibitor. On day 8, the supernatants from transformed B cells were used to screen for the presence of antigen-reactive antibodies against H7 HA from A/Shanghai/2/2013 (H7N9) using a capture ELISA. Cells from the wells containing B cells secreting HA-reactive antibodies were fused with HMMA2.5 myeloma cells using an

ECM 2001 electro cell manipulator (BTX), and human hybridomas were selected in medium with hypoxanthine-aminopterin-thymidine solution containing ouabain. The hybridomas were cloned by flow cytometric sorting of single cells into 384-well plates and then expanded in culture. The selected cell line was grown in hybridoma growth medium (ClonaCell-HY medium E from STEMCELL Technologies) and then switched to serum-free medium (GIBCO Hybridoma-SFM, Thermo Fisher Scientific) for antibody expression. IgG from the hybridoma cell line supernatants was purified by affinity chromatography using Mab SelectSure columns (GE Healthcare Life Sciences). Purified IgG generated from hybridomas was used for all in vitro and in vivo studies.

ELISA. To determine EC_{50} concentrations for binding, we performed ELISAs using 384-well plates that were coated overnight at 1 μg/mL with the recombinant HA protein of interest. The plates then were blocked with 50 μL of 5% non-fat dry milk and 0.1% Tween-20 in D-PBS (ELISA buffer) for 1 hr at RT. The plates were washed and three-fold dilutions of the mAb in ELISA buffer at a starting concentration of 10 μg/mL were added to the wells and incubated for an hour. The plates were washed and 25 μL of ELISA buffer containing a 1:4,000 dilution of anti-human IgG alkaline phosphatase conjugate (Meridian Life Science, W99008A) was added. After a final wash, 25 μL of phosphatase substrate solution (1 mg/mL p-nitrophenol phosphate in 1 M Tris aminomethane) was added to the plates, incubated for 1 hr and the optical density values were measured at 405 nm wavelength on a BioTek plate reader. The plates were washed 3 times between each step with PBS containing 0.05% Tween-20. Each dilution was performed in triplicate, and the EC_{50} values were calculated in Prism software (GraphPad) using non-linear regression analysis. Each experiment was conducted twice independently.

Microneutralization assay. Neutralization potential of H7-200 IgG was determined by microneutralization and HAI assays, as previously described (3). Briefly, 2-fold serial dilutions of each antibody in viral growth medium (plain DMEM supplemented with 2 μg/mL of TPCK-trypsin (Sigma, T1426) and penicillin, streptomycin (Gibco, 10378-016)) were mixed with an equivalent volume of viral growth medium containing 100 $TCID_{50}$ of virus. Antibody and virus were incubated for 1 hr at RT. The MDCK cell monolayer cultures were washed twice with 100 μL PBS containing 0.1% Tween-20, and the virus-antibody mixture then was added to cells and incubated for 24 hours at 37°C. After incubation, cells were washed and fixed with 100 μL of 80% methanol/20% PBS. The presence of influenza nucleoprotein in the fixed cells was determined by ELISA using a 1:8,000 dilution of mouse anti-NP antibody (BEI Resources, NR-4282) as the primary antibody and a 1:4,000 dilution of goat anti-mouse alkaline phosphate conjugate as the secondary antibody (Novex, A16014). Each dilution was tested in triplicate and neutralization curves were graphed using GraphPad Prism.

Negative stain electron microscopy. H7-200 Fabs were incubated with uncleaved H7 SH13 HA trimer for 20 seconds at 5 times molar excess of Fab. The complex was added to carbon-coated 400 mesh cooper grids and stained with 2% uranyl formate. Micrographs were collected on a 120kv Tecnai Spirit microscope with a 4kx4k TemCam F416 camera using Leginon. Images were processed within Appion (4). Particles were selected with DoGpicker (5) and 2D classes were generated with MSA/MRA(6). Particles were colored in Photoshop.

In vivo protection study. Mice were housed in individually ventilated cage racks with negative pressure ventilation and air filtering (Allentown, Inc., Allentown, NJ). To assess protective efficacy of the mAb, female 18-20 g BALB/c mice (Charles River Laboratories, Wilmington, MA) were inoculated by the intraperitoneal (i.p.) route with a 200-µg dose of H7-200 or a control antibody. Human anti-dengue virus mAb DENV 2D22 served as a mock control treatment, while a recombinant form of human mAb rCR9114 directed to the HA stem region served as a positive control. In ABSL-2 facilities, ketamine-xylazine anesthetized mice were inoculated by the intranasal (i.n.) route at 24 hours after the mAb treatment with 10^4 focus forming units (~4 x LD_{80}) of H7N9 A/Shanghai/2/2013 IDCDC-RG32A in 50 µL of sterile PBS. Mice were weighed and monitored daily for body weight change and signs of disease for 14 days, and those losing over 30% of initial body weight were humanely euthanized as per IACUC requirements. This study was conducted in the AAALAC-accredited laboratory animal research center of Vanderbilt University Medical Center in accordance with the approval of the Institutional Animal Care and Use Committee of Vanderbilt University Medical Center. The clinical symptoms were scored as follows: 0 - at healthy state, 1 - signs of ruffled fur and/or back arching, 2 - extensive fur ruffling and hunching posture, 3 – as above and little mobility or lethargy, 4 - moribund stage.

Competition-binding groups. Biolayer interferometry on an Octet Red instrument (FortéBio) was used to perform competition-binding assays. We loaded the H7 HA1 from A/Shanghai/2/2013 H7N9 with 6xHis-tag onto Anti-Penta-HIS biosensors (FortéBio, 18-5120) at a concentration of 10 µg/mL, and when tested binding of two successively applied mAbs at 50 µg/mL concentration. Antigen and Abs dilutions were made in 1X Kinetics Buffer (FortéBio, 18-5032). The mAbs were defined as competing if the first Ab reduced binding of the second Ab by more than 60 percent.

The mAbs were defined as non-competing if the first Ab reduced binding of the second by less than 30 percent.

Peptide fragmentation and deuterium exchange mass spectrometry. To maximize peptide probe coverage, the optimized quench condition was determined prior to deuteration studies. The HA head domain was diluted with buffer of 8.3 mM Tris, 150 mM NaCl, in H_2O, pH 7.5) at 0 °C and then quenched with 0.8% formic acid (v/v) containing various concentration of GuHCl (0.8 - 6.4 M) and Tris(2-carboxyethyl)phosphine (TCEP) (0.1 or 1.0 M). After incubating on ice for 5 min, the quenched samples were diluted 3-fold with 0.8% formic acid (v/v) containing 16.6% (v/v) glycerol and then were frozen at -80°C until they were transferred to the cryogenic autosampler. Using the quench buffer of 6.4 M GuHCl, 1 M TCEP in 0.8% formic acid gave an optimal peptide coverage map. The samples later were thawed automatically on ice and then immediately passed over an AL-20-pepsin column (16 μL bed volume, 30 mg/mL porcine pepsin [Sigma]). The resulting peptides were collected on a C18 trap and separated a C18 reversed phase column (0.2 x 50 mm, Optimize Technologies Inc) running a linear gradient of 0.046% (v/v) trifluoroacetic acid, 6.4% (v/v) acetonitrile to 0.03% (v/v) trifluoroacetic acid, 38.4% (v/v) acetonitrile over 30 min with column effluent directed into an Orbitrap Elite mass spectrometer (Thermo-Fisher Scientific). Data were acquired in both data-dependent MS:MS mode and MS1 profile mode. Proteome Discoverer software (ThermoFisher Scientific Inc.) was used to identify the sequence of the peptide ions. HDEXaminer software (Sierra Analytics Inc., Modesto, CA) was used for the analysis of the mass spectra. Fab bound HAs were prepared by mixing H7-200 Fab with monomeric H7 head domain at a 1:1.1 (HA:Fab) stoichiometric ratio. The mixtures were incubated at 25 °C for 30 min. All functionally deuterated samples, with the exception of the equilibrium-

deuterated control, and buffers were pre-chilled on ice and prepared in the cold room. Functional deuterium-hydrogen exchange reaction was initiated by diluting free HA or antibody-bound HA stock solution with D_2O buffer (8.3 mM Tris, 150 mM NaCl, in D_2O, pDREAD 7. 5) at a 1:2 vol/vol ratio. At 10 sec, 100 sec and 1,000 sec, the quench solution was added to the respective samples, and incubated on ice for 5 minutes, then diluted with 3-fold with 0.8 % formic acid before freezing at -80 °C. In addition, nondeuterated samples, equilibrium-deuterated back-exchange control samples were prepared as previously described (7, 8). The centroids of the isotopic envelopes of nondeuterated, functionally deuterated, and fully deuterated peptides were measured using HDEXaminer, and then converted to corresponding deuteration levels with corrections for back-exchange (9).

Crystallization, data collection, and structure determination. Purified H7N9 HA1 and H7-200 Fab were mixed in a molar ratio of 1:2. The mixture was incubated at room temperature for ~ 10 minutes, and then the antigen-antibody complex was purified from the mixture using a HiLoad® 16/600 Superdex® 200 size-exclusion column (GE Healthcare Life Sciences). The purified complex of H7N9 HA1 and H7-200 Fab was concentrated to ~ 10 mg/mL in a buffer of 20 mM Tris-HCl pH 7.5, 50 mM NaCl. Extensive crystallization screening was performed with the concentrated sample using a mosquito® XTAL3 crystallization robot (TTP Labtech), and subsequent optimization was carried out with a dragonfly® crystal screen optimizer (TTP Labtech). H7-200/H7-HA1 complex was crystallized in 0.1 M sodium citrate pH 6.0, 10% isopropanol, 22% PEG 400. The crystals were flash frozen in liquid nitrogen with 25% PEG 400 as the cryoprotectant. Diffraction data were collected at the Advanced Photon Source LS-CAT beamline 21-ID-G. The data were processed and integrated with XDS data processing software package

(10), and scaled with SCALA (11). The crystal structure of the complex was solved by molecular replacement with the software Phaser (12) using the crystal structure of H7N9 Shanghai head domain (PDB ID: 4N5J) and the crystal structure of human anti-Marburg virus Fab MR78 (PDB ID: 5JRP) as the searching models. Iterative refinement and manual rebuild of the crystal structure were done with Phenix and coot (13, 14). The data collection and refinement statistics are shown in Table S1. All structure figures were made using the molecular graphics software PyMOL (Shrodinger).

Supplemental References

1. Skowronski DM, Chambers C, Gustafson R, Purych DB, Tang P, Bastien N, et al. Avian influenza A(H7N9) virus infection in 2 travelers returning from China to Canada, January 2015. *Emerg Infect Dis.* 2016;22(1):71-4.

2. Smith SA, and Crowe JE, Jr. Use of human hybridoma technology to isolate human monoclonal antibodies. *Microbiol Spectr.* 2015;3(1):AID-0027-2014.

3. Thornburg NJ, Zhang H, Bangaru S, Sapparapu G, Kose N, Lampley RM, et al. H7N9 influenza virus neutralizing antibodies that possess few somatic mutations. *J Clin Invest.* 2016;126(4):1482-94.

4. Lander GC, Stagg SM, Voss NR, Cheng A, Fellmann D, Pulokas J, et al. Appion: An integrated, database-driven pipeline to facilitate EM image processing. *J Struct Biol.* 2009;166(1):95-102.

5. Voss NR, Yoshioka CK, Radermacher M, Potter CS, and Carragher B. DoG Picker and TiltPicker: software tools to facilitate particle selection in single particle electron microscopy. *J Struct Biol.* 2009;166(2):205-13.

6. Ogura T, Iwasaki K, and Sato C. Topology representing network enables highly accurate classification of protein images taken by cryo electron-microscope without masking. *J Struct Biol.* 2003;143(3):185-200.

7. Hsu S, Kim Y, Li S, Durrant ES, Pace RM, Woods VL, Jr., et al. Structural insights into glucan phosphatase dynamics using amide hydrogen-deuterium exchange mass spectrometry. *Biochemistry.* 2009;48(41):9891-902.

8. Li S, Tsalkova T, White MA, Mei FC, Liu T, Wang D, et al. Mechanism of intracellular cAMP sensor Epac2 activation: cAMP-induced conformational changes identified by amide hydrogen/deuterium exchange mass spectrometry (DXMS). *J Biol Chem.* 2011;286(20):17889-97.

9. Zhang Z, and Smith DL. Determination of amide hydrogen exchange by mass spectrometry: a new tool for protein structure elucidation. *Protein Sci.* 1993;2(4):522-31.

10. Kabsch W. XDS. *Acta Crystallogr D Biol Crystallogr.* 2010;66(Pt 2):125-32.

11. Winn MD, Ballard CC, Cowtan KD, Dodson EJ, Emsley P, Evans PR, et al. Overview of the CCP4 suite and current developments. *Acta Crystallogr D Biol Crystallogr.* 2011;67(Pt 4):235-42.

12. McCoy AJ, Grosse-Kunstleve RW, Adams PD, Winn MD, Storoni LC, and Read RJ. Phaser crystallographic software. *J Appl Crystallogr.* 2007;40(Pt 4):658-74.

13. Adams PD, Afonine PV, Bunkoczi G, Chen VB, Davis IW, Echols N, et al. PHENIX: a comprehensive Python-based system for macromolecular structure solution. *Acta Crystallogr D Biol Crystallogr.* 2010;66(Pt 2):213-21.

14. Emsley P, and Cowtan K. Coot: Model-building tools for molecular graphics. *Acta Crystallogr D Biol Crystallogr.* 2004;60(Pt 12 Pt 1):2126-32.

SUPPLEMENTAL TABLES

Table S1. Sequence features of the variable genes encoding human mAb H7-200

Chain	V gene	D gene	J gene	CDR3 amino acids	Amino acid sequence identity of the recombined variable gene to the inferred germline genes	
					# amino acids identical/total	% amino acid identity
Heavy	*IGHV4-61*02*	*IGHD5-18*01*	*IGHJ6*03*	ARESLWNPDYYYYMDV	119/131	90.8
Light	*IGKV1-39*01 or IGKV1D-39*01*	*na*	*IGKJ2*01*	QQSYSVPYT	115/123	93.5

na - indicates *not applicable*

Table S2. Cross-reactivity of H7-200, H7.5 and FluA-20 mAbs, Related to Figure 1

mAb	EC_{50} (ng/mL) for binding, to indicated HA antigens from Group 2									
	H7									H15
	SH13 HA1	SH13 HA	BC15 HA	HN16 HA	GD16 HA	EN96 HA	NL03 HA	rCA04 HA	NY03 HA	wt/WA 79 HA
H7-200	7.1	7.8	6.5	7.8	13	7.4	5.7	5.3	8.9	8.2
H7.5	nd	4.8	5.6	5.1	12	5.9	4.9	5.2	4.3	>
FluA-20	nd	40	55	56	50	11	9.2	36	>	11

The > symbol indicates binding was not detected when tested at concentrations as high as 10 μg/mL.

“nd” indicates not determined.

Table S3. Cross-reactivity of H7-200, H7.5 and FluA-20 mAbs, Related to Figure 1

mAb	Optical density (405 nm) at IgG concentration of 10 µg/mL																						
	HA antigens from Group 2													HA antigens from Group 1									
	H7								H15	H3			H4	H6	H11	H2	H5		H1			H8	H12	H9
	SH13	BC15	HN16	GD16	EN96	NL03	rCA04	NY03	wt/WA79	HK68	CA04	SW13	d/CS56	TW13	d/MP74	SG57	VN04	IN05	PR34	TX91	CA09	t/OT68	d/AB76	HK99
H7-200	3.6	3.6	3.7	3.7	3.7	3.7	3.7	3.7	3.7	0.1	0.1	0.1	0.1	0.1	0.1	0.1	0.1	0.1	0.1	0.1	0.1	0.1	0.1	0.2
H7.5	3.7	3.6	3.7	3.7	3.7	3.7	3.7	3.8	0.2	0.1	0.1	0.1	0.1	0.1	0.1	0.1	0.1	0.2	0.1	0.1	0.1	0.1	0.1	0.2
FluA-20	3.6	3.5	3.7	3.7	3.7	3.7	3.7	0.2	3.8	3.7	3.6	3.6	3.7	3.0	1.4	2.3	1.1	3.5	3.7	3.4	0.5	3.7	3.6	3.7

Table S4. Data collection and refinement statistics for the crystals of H7-200/H7-HA1 complexes, Related to Figure 3

Data collection	
Crystal	H7-200/H7-HA1
PDB ID	6UIG
Wavelength (Å)	0.97857
Space group	$P4_322$
Unit cell dimensions	
a, b, c (Å)	156.5, 156.5, 229.1
α, β, γ	90, 90, 90
Resolution (Å)	49.82 – 3.20
Unique reflections	47601 (6843)
Redundancy	5.5 (5.5)
Completeness (%)	99.9 (100.0)
R_{merge} (%)	9.7 (60.7)
I/σ(I)	11.3 (2.7)
Refinement statistics	
R_{factor} (%)	20.7
R_{free} (%)	23.4
R.m.s.d. (bond) (Å)	0.0020
R.m.s.d. (angle) (deg)	0.559
Ramachandran plot	
Favored (%)	96.08
Allowed (%)	3.77
Outliers (%)	0.15

$R_{merge} = \Sigma \Sigma |I_{hkl} - I_{hkl(j)}|/\Sigma I_{hkl}$, where $I_{hkl(j)}$ is the observed intensity and I_{hkl} is the final average intensity.
$R_{work} = \Sigma ||Fobs| - |Fcalc||/\Sigma |Fobs|$ and $R_{free} = \Sigma ||Fobs| - |Fcalc||/\Sigma |Fobs|$, where R_{free} and R_{work} are calculated using a randomly selected test set of 5% of the data and all reflections excluding the 5% test set, respectively. Numbers in parentheses are for the highest resolution shell.

Table S5. BC15 H7 HA contact residues with antibody H7-200 and conservation in other influenza HA subtypes and strains, Related to Figure 3

Sub-type	Strain	Contact residues in HA epitope																			
		101	103	104	163	182	184	199	200	201	208	209	210	211	212	213	214	215	216	231	233
H7N9	**BC15**	**K**	**V**	**N**	**Q**	**I**	**H**	**N**	**K**	**L**	**N**	**Y**	**Q**	**Q**	**S**	**F**	**V**	**P**	**S**	**D**	**H**
H7N9	SH13	·	·	·	.	·	·	·	·	·	·	·	·	·	·	·	·	·	·	·	·
	HN16	·	·	·	·	·	·	·	·	·	·	·	·	·	·	·	·	·	·	·	·
	GD16	·	·	·	·	·	·	·	·	·	·	·	·	·	·	·	·	·	·	·	·
H7N7	EN96	·	·	·	·	·	·	·	·	·	·	·	·	·	·	·	·	·	·	·	·
	NL03	·	·	·	·	·	·	·	·	·	·	·	·	·	·	·	·	·	·	·	·
H7N3	rCA04	·	T	·	·	V	·	·	·	·	K	·	·	·	·	·	T	·	.	·	·
H7N2	NY03	R	T	·	·	V	·	·	·	·	K	·	·	·	·	·	T	·	N	·	·
H15N9	wtWA79	R	T	·	·	V	·	·	·	·	K	·	·	·	·	·	S	·	.	·	·
H3N2	HK68	D	P	D	V	V	·	S	G	R	R	S	·	·	T	I	I	·	N	S	Y
	CA04	D	P	D	A	V	·	S	G	R	R	S	·	·	T	V	I	·	N	S	Y
	SW13	D	P	D	A	V	·	S	G	R	R	S	·	·	A	V	I	·	N	S	Y
H4N6	dCS56	D	P	E	L	V	·	P	G	R	T	S	·	T	.	V	.	·	N	S	Y
H6N1	TW13	V	N	E	V	V	·	D	.	Y	S	M	N	F	A	K	S	·	E	.	Y
H11N9	dMP74	T	E	.	V	V	·	.	S	Y	S	.	N	R	R	.	T	·	E	T	Y
H2N2	SG57	S	N	D	V	V	·	G	T	Y	T	L	N	K	R	S	T	·	D	E	S
H5N1	VN04	D	N	D	T	·	·	T	T	Y	T	L	N	·	R	L	·	·	R	E	F
	IN05	S	N	D	T	·	·	T	T	Y	T	L	N	·	R	L	·	·	K	E	F
H1N1	PR34	D	I	D	K	·	·	·	A	Y	N	Y	N	R	R	·	T	·	E	N	Y
	TX91	Y	A	D	N	V	·	·	A	Y	H	.	S	R	R	·	T	·	E	N	Y
	CA09	D	I	D	K	·	·	D	T	Y	R	.	S	K	K	·	K	·	E	N	Y
H8N4	tOT68	S	E	·	F	·	·	.	T	·	T	I	N	R	·	·	Q	·	N	·	Y
H12N5	dAB76	S	E	·	V	·	·	D	T	·	E	I	N	R	·	·	K	·	N	·	Y
H9N2	HK99	N	E	·	V	·	·	D	T	T	D	L	N	R	T	·	K	·	V	·	Y

The dot symbol (.) in the table indicates identity at that contact residue position with BC15 H7.

Red color indicates an amino acid that differs from the BC15 H7 HA amino acid at that contact residue position.

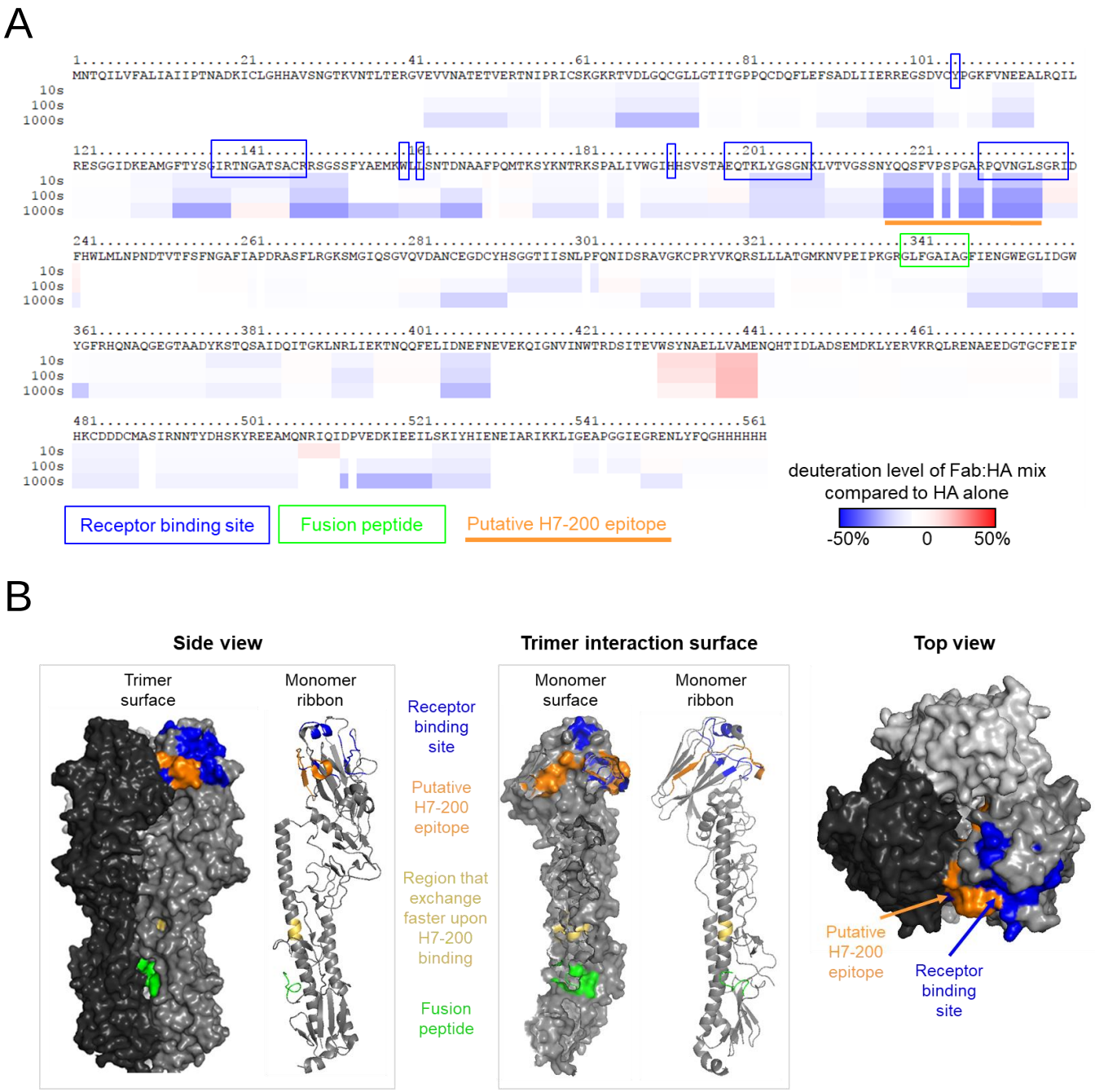

Figure S1. Hydrogen deuterium exchange mass spectrometry data to determine the putative epitope on H7 HA for binding by mAb H7-200.
A) Influence of mAb H7-200 on deuteration level of soluble trimer H7 HA (SH13). HDX-MS with H7-200 Fab and H7 HA identified a putative epitope for H7-200 at the trimer-interface. The amino acid sequence of the H7 HA is shown with a ribbon diagram indicating differences in deuterium uptake. Blue colors indicating slower deuterium exchange in the presence of H7-200 Fab, while red colors indicate faster deuterium exchange in the presence of H7-200 Fab. Data are shown for 10 s, 100 s, or 1,000 s of deuterium labeling. HA residues are numbered from the start of the H7 HA construct. **B) Putative epitope for mAb H7-200 on H7 HA based on deuteration levels.** The H7-200 putative epitope (region that exchanges slower upon H7-200 binding) is shown in orange on the ribbon or surface representation of the H7 (A/Shanghai/2/2013) HA monomer or trimer. The region in the stem that exchanges faster upon H7-200 binding is indicated in yellow. For reference, the receptor binding site is indicated in blue and the fusion peptide in green.

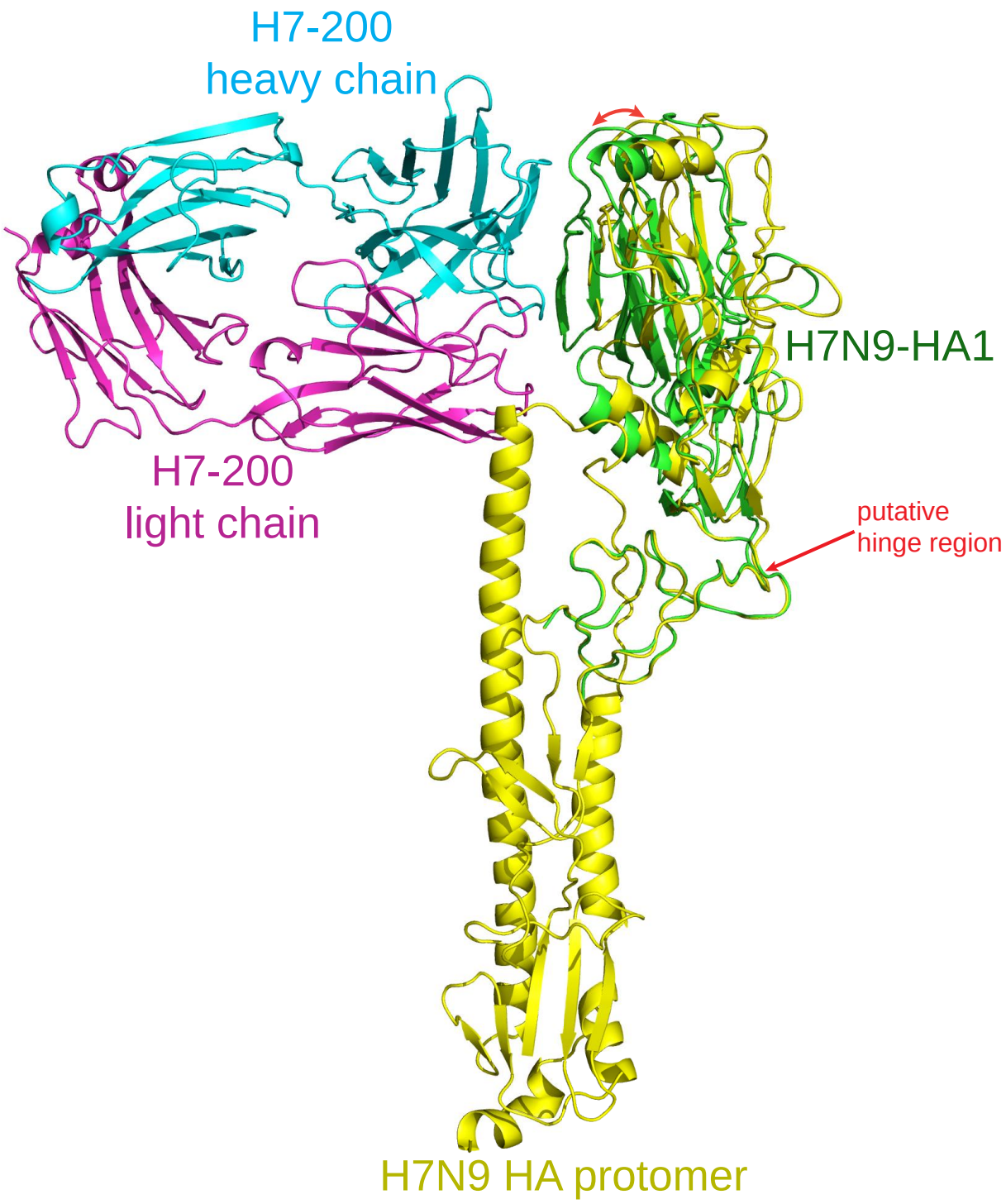

Figure S2. Movement within the HA head domain upon binding of H7-200. Superimposition of the vestigial esterase domain of HA1 in the complex of H7-200 [heavy chain cyan, light chain pink] and H7.HA1 (green) with that in the apo H7N9 HA trimer (yellow, based on PDB ID: 4N5J) indicated that the orientations of receptor binding domains vary significantly relative to the vestigial esterase domain. There appears to be a minor hinge function for rigid body rotations located between the receptor binding domain and the vestigial esterase domain (indicated by red arrow).